

# Lawrence Berkeley National Laboratory

## Recent Work

**Title**

DIFFUSION OF IRON INTO SINGLE-CRYSTAL MgO

**Permalink**

<https://escholarship.org/uc/item/99f4c3bz>

**Author**

Blank, Stuart L.

**Publication Date**

1963-11-15

UCRL-11073

**University of California**  
**Ernest O. Lawrence**  
**Radiation Laboratory**

**TWO-WEEK LOAN COPY**

*This is a Library Circulating Copy  
which may be borrowed for two weeks.  
For a personal retention copy, call  
Tech. Info. Division, Ext. 5545*

**DIFFUSION OF IRON INTO SINGLE-CRYSTAL MgO**

**Berkeley, California**

## **DISCLAIMER**

This document was prepared as an account of work sponsored by the United States Government. While this document is believed to contain correct information, neither the United States Government nor any agency thereof, nor the Regents of the University of California, nor any of their employees, makes any warranty, express or implied, or assumes any legal responsibility for the accuracy, completeness, or usefulness of any information, apparatus, product, or process disclosed, or represents that its use would not infringe privately owned rights. Reference herein to any specific commercial product, process, or service by its trade name, trademark, manufacturer, or otherwise, does not necessarily constitute or imply its endorsement, recommendation, or favoring by the United States Government or any agency thereof, or the Regents of the University of California. The views and opinions of authors expressed herein do not necessarily state or reflect those of the United States Government or any agency thereof or the Regents of the University of California.

UCRL-11073  
UC-25 Metals,  
Ceramics and  
Materials  
TID-4500 (24th Ed.)

UNIVERSITY OF CALIFORNIA  
Lawrence Radiation Laboratory  
Berkeley, California

AEC Contract No. W-7405-eng-48

DIFFUSION OF IRON INTO SINGLE-CRYSTAL MgO

Stuart L. Blank

(M. S. Thesis)

November 15, 1963

Printed in USA. Price 75 cents. Available from the  
Office of Technical Services  
U. S. Department of Commerce  
Washington 25, D.C.

DIFFUSION OF IRON INTO SINGLE-CRYSTAL MgO

Contents

Abstract . . . . .	v
I. Introduction . . . . .	1
II. Background Material . . . . .	2
A. Fick's Laws . . . . .	3
B. The Temperature Dependence of the Diffusion Coefficient . . . . .	5
C. Diffusion in Ionic Crystals . . . . .	5
III. Procedure and Apparatus . . . . .	7
A. Electron Microprobe Analyzer . . . . .	9
IV. Results and Discussion of Results . . . . .	12
V. Conclusions . . . . .	23
Acknowledgments . . . . .	24
Appendix . . . . .	25
Footnotes and References . . . . .	26

## DIFFUSION OF IRON INTO SINGLE-CRYSTAL MgO

Stuart L. Blank

Lawrence Radiation Laboratory  
University of California  
Berkeley, California

November 15, 1963

### ABSTRACT

MgO single crystals were packed in iron powder and heated in a vacuum at 1150, 1250, and 1350°C. Concentration-vs-penetration profiles were determined by using the electron microprobe analyzer. The interdiffusion coefficient  $D$  is found to be concentration dependent in the range 1 to 22 at. % Fe. At 1150°C we have

$$D = 8.1 \times 10^{-12} e^{0.150[\text{Fe}]} \text{ cm}^2/\text{sec},$$

at 1250°C

$$D = 1.60 \times 10^{-11} e^{0.173[\text{Fe}]},$$

and at 1350°C

$$D = 2.40 \times 10^{-11} e^{0.190[\text{Fe}]},$$

The apparent activation energy for diffusion increases with the iron concentration.

At an iron concentration  $C = 5$  at. %, we have

$$D = 6.34 \times 10^{-7} \exp(-29600/RT),$$

at  $C = 10$

$$D = 4.49 \times 10^{-6} \exp(-32900/RT),$$

$C = 15$

$$D = 5.04 \times 10^{-5} \exp(-37700/RT),$$

and at  $C = 20$

$$D = 8.40 \times 10^{-4} \exp(-43500/RT).$$

## I. INTRODUCTION

Refractory inorganic oxides have recently been under investigation because of the need for materials with specific physical properties such as low vapor pressure, high melting temperature, and controlled impurity content. Oxides such as  $\text{Al}_2\text{O}_3$  and  $\text{MgO}$  have the advantages of high melting temperatures, high heats of formation (indicating great stability), good mechanical strength, great abundance, and good optical characteristics. Since for more advanced applications these oxides must be modified (by doping, etc.), to give them certain physical properties, the fundamentals of the solid-state reactions involving these materials should be understood.

Diffusion plays a most important role in almost all high-temperature solid-state reactions. An accurate knowledge and understanding of the diffusivities of various components in these oxides is therefore of great practical and theoretical value. In this study we investigate the couple iron- $\text{MgO}$ , in order to obtain quantitative data regarding the interdiffusion coefficient.



## II. BACKGROUND MATERIAL

Diffusion plays an extremely important role in such processes as creep, sinterability, electrical conductivity, and oxidation.<sup>1, 2</sup> Because of the primary role of diffusion in solid-state reactions, many reviews have been written on the subject.<sup>3-7</sup> Investigators have proposed various mechanisms for diffusion in solids; some of the most significant are

- (a) direct interchange of positions,
- (b) movement through interstitial positions,
- (c) ring mechanisms,

and

- (d) vacancy mechanisms.

The direct-interchange and ring mechanisms result in the exchange of positions between atoms in a crystalline solid. These have not been experimentally observed to occur in any real system. The interstitial mechanism requires formation of Frenkel defects, in which atoms move from normal lattice positions into interstitial sites. The movement of an atom or ion from one interstitial site to another is termed interstitial diffusion.

The most widely accepted mechanism for diffusion in ionic solids is the vacancy mechanism (which is also accepted by the author as being the most likely mechanism). Atoms may diffuse by jumping from a normal lattice position into a vacancy, or empty lattice site. At any temperature above absolute zero, the lattice of an ionic crystal contains some thermally created vacancies. Vacancies may also be created chemically. In MgO, vacancies may be chemically formed by introducing cations of different valence than those of the matrix material; the presence of iron in the  $\text{Fe}^{+3}$  state would cause cation vacancies.

In a stoichiometric lattice such as MgO, if no point defects were present there could be no bulk diffusion. However, in order for diffusion to proceed in stoichiometric ionic crystals, some source of point defects must exist. Both thermally and chemically caused vacancies are present in the  $\text{Fe}_x\text{O}$ -MgO system.

### A. Fick's Laws

Fick treated diffusion on a quantitative basis by adopting the mathematical equations used for heat flow for use in describing the diffusion process.<sup>3</sup> For a single phase at constant temperature and pressure, diffusion occurs in a direction that equalizes the activity gradient. The quantity of material that diffuses past a unit area normal to the diffusion direction in unit time is proportional to the activity gradient. Because it is difficult to determine the activity gradient accurately in various diffusion experiments, concentration gradients are usually used in the diffusion equations. Fick's first law states that the driving force for the diffusion process is the chemical concentration gradient

$$J = - \left( D \frac{\partial c}{\partial x} \right), \quad (1)$$

where  $J$  = flux,  $c$  = concentration per unit volume,  $x$  = distance in diffusion direction, and  $D$  = diffusion coefficient ( $\text{cm}^2/\text{sec}$ ).

The change of concentration of the diffusing substance with time is given by Fick's second law,

$$\frac{\partial c}{\partial t} = \frac{\partial}{\partial x} \left( D \frac{\partial c}{\partial x} \right). \quad (2)$$

If it is assumed that the diffusion coefficient  $D$  is constant, solutions to this equation may be found for various boundary conditions. Rigorous solutions of this equation are usually not available when  $D$  varies with concentration; therefore, to obtain numerical values graphical solutions are usually used. Boltzmann,<sup>3, 6, 8</sup> in 1894, showed that for certain boundary conditions, provided that  $D$  is a function of  $c$  only,  $c$  may be expressed in terms of a single variable  $x/2(t)^{1/2}$ . As a result, Eq. (2) can be reduced to an ordinary differential equation if a new variable,  $\eta$ , is introduced where

$$\eta = \frac{1}{2} x/t^{1/2}. \quad (3)$$

We then obtain

$$\frac{\partial c}{\partial x} = \frac{1}{2t^{1/2}} \frac{dc}{d\eta} \quad (4)$$

and

$$\frac{\partial c}{\partial t} = - \frac{x}{4t^{3/2}} \frac{dc}{d\eta} ; \quad (5)$$

therefore, we get

$$\frac{\partial}{\partial x} \left( D \frac{\partial c}{\partial x} \right) = \frac{\partial}{\partial x} \left( \frac{D}{2t^{1/2}} \frac{dc}{d\eta} \right) = \frac{1}{4t} \frac{d}{d\eta} \left( D \frac{dc}{d\eta} \right). \quad (6)$$

Equation (2) results in

$$- 2 \eta \frac{dc}{d\eta} = \frac{d}{d\eta} \left( D \frac{dc}{d\eta} \right), \quad (7)$$

which is an ordinary differential equation in  $c$  and  $\eta$ . If two infinite media are brought together at  $t = 0$ , the diffusion coefficient and its concentration dependence may be deduced from the concentration-vs-penetration curves observed at some known time. The boundary conditions are

$$C = \text{infinity}, \quad x < 0, \quad t = 0,$$

and

$$C = 0, \quad x > 0, \quad t = 0,$$

where  $C$  is the concentration of the component in which we have interest, and  $x = 0$  is the position of the original interface of the two components at  $t = 0$ . Integration of Eq. (7) with respect to  $\eta$  results in

$$-2 \int_0^{c_1} \eta dc = \left[ D \frac{dc}{d\eta} \right]_{C=0}^{C=C_1} = \left( D \frac{dc}{d\eta} \right)_{C=C_1}, \quad (8)$$

where  $C_1$  = any value of  $C$  between zero and infinity. Rearranging Eq. (8) and introducing  $x$  and  $t$ , we obtain

$$D_{C=C_1} = - \frac{1}{2t} \frac{dx}{dc} \int_0^{C_1} x dc. \quad (9)$$

Equation (9) gives the diffusion coefficient ( $D$ ) for any value of  $C$ .

When the diffusion coefficient is not constant, many types of concentration-vs-penetration curves are obtainable.<sup>3</sup> For our purposes, the most interesting type is one having a plateau-shaped curve with a high concentration gradient near the  $C = 0$  boundary of the system. This type of gradient, which allows a visible boundary to be observed advancing into the host lattice, has been observed by this author as well as by previous authors.<sup>9-11</sup>

#### B. The Temperature Dependence of the Diffusion Coefficient

The temperature dependence of the diffusion coefficient can usually be expressed in terms of the Arrhenius equation,<sup>5</sup> where  $D = D_0 \exp(-Q/RT)$ . Here we have

$$D_0 = \text{diffusivity constant}$$

and

$$Q = \text{energy of activation.}$$

The temperature dependence may also be written in terms of the absolute reaction-rate equation<sup>12</sup>

$$D = \lambda^2 \frac{kT}{h} \exp\left(\frac{\Delta S_0^*}{R}\right) \exp\left(\frac{-\Delta H_0^*}{RT}\right), \quad (10)$$

where

$\lambda$  = the jump distance,

$T$  = temperature in  $^\circ\text{K}$ ,

$k$  = Boltzmann's constant,

$h$  = Planck's constant,

$S_0^*$  = entropy of activation,

$H_0^*$  = enthalpy of activation,

and

$R$  = universal gas constant.

#### C. Diffusion in Ionic Crystals

Most investigators of diffusion in ionic crystals have been concerned with self-diffusion of various components, or with inter-diffusion reactions between ionic compounds. In this discussion we are primarily concerned with interdiffusion reactions. Jost has

stated that when diffusion occurs in ionic compounds, the mobility of the larger anions is very much smaller than that of the cations.<sup>4</sup> The work of Carter on the interdiffusion of metallic oxides (MgO, Al<sub>2</sub>O<sub>3</sub>) has confirmed this assumption.<sup>9</sup> According to Crank,<sup>3</sup> even though the diffusion coefficient in ionic solids is measured in the same way as in metals, mass flow usually does not occur; therefore, a Kirkendall effect is not observed.

Self-diffusion measurements of Fe<sup>+2</sup> in Fe<sub>x</sub>O have been made by a number of authors.<sup>13, 14</sup> Wustite (Fe<sub>x</sub>O) is an ionic compound having a rock-salt type of structure.<sup>15</sup> The oxygen ions are in a close-packed cubic arrangement, with the iron ions occupying the octahedral positions. It is found that wustite is not a stoichiometric compound, always containing a deficiency of iron.<sup>7</sup> Because of the necessity of retaining electrical neutrality in the ionic crystal, the nonstoichiometric wustite must contain some concentration of Fe<sup>+3</sup>, the ratio of trivalent iron to vacancy concentration being 2/1.

Magnesium oxide or periclase is similar to Fe<sub>x</sub>O in that it also has the rock-salt structure. Magnesium oxide, however, exists as a stoichiometric compound.<sup>16</sup> The only vacancies present in the MgO lattice are caused either by thermal means or by impurity cations having valences other than two. Both MgO and wustite have the same crystal structure, similar lattice parameters, and similar ionic radii. We would therefore expect to find a continuous solid solution between them at high temperatures, and a continuous solid solution has been reported for them.<sup>18</sup> Brynstad and Flood have observed that the ratio of Fe<sup>+3</sup>/Fe<sup>+2</sup> in a solid solution of Fe<sub>x</sub>O·MgO decreases with increasing concentration of magnesium ions.<sup>19</sup> This same phenomenon has also been confirmed by Rigby.<sup>9</sup> The diffusion of iron in the Fe<sub>x</sub>O-MgO system is thought to occur by the vacancy mechanism.

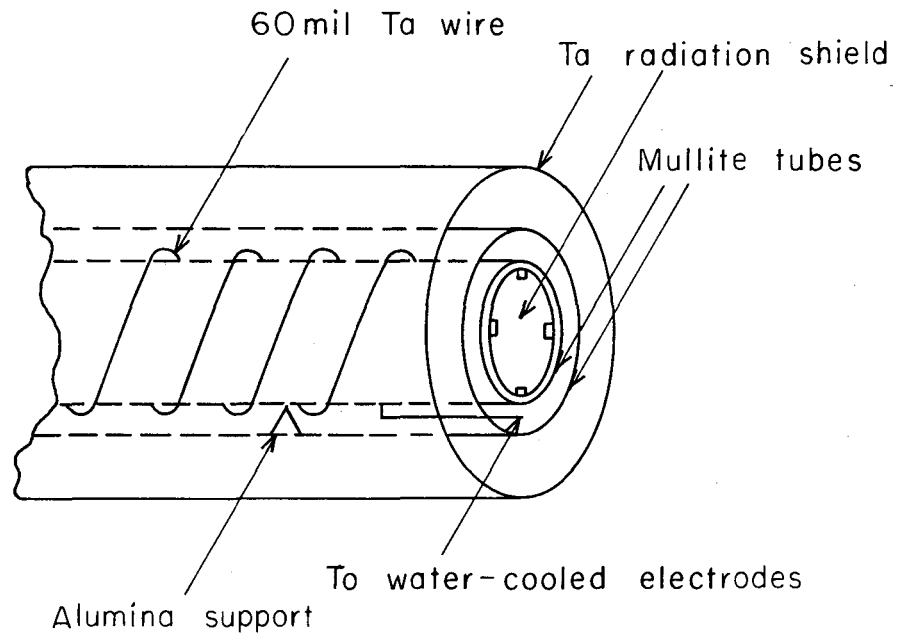
### III. PROCEDURE AND APPARATUS

A high-temperature vacuum furnace was constructed in which the diffusion runs were made. The furnace consisted of a mullite tube around which was wound 60-mil tantalum wire (Fig. 1). The ends of the tube were fitted with tantalum radiation shields as was the entire length of the furnace. A bell-jar vacuum system completely enclosed the furnace. The base plate of the furnace and the electrodes that introduced power to the furnace were both water cooled. An oil-diffusion pump backed by a high-capacity mechanical pump was used to obtain pressures in the range of  $10^{-6}$  torr. Pressure was measured by a thermocouple vacuum gauge in the high-pressure region and by an ion gauge in the low-pressure region. A proportional-band controller that fed a silicon-controlled rectifier circuit regulated the temperature. Control sensing was accomplished by use of a thermocouple placed near the diffusion sample. A separate thermocouple placed directly in contact with the sample measured the actual sample temperature; this was recorded on a recording potentiometer.

A recrystallized alumina crucible was first filled with iron powder and heated in the vacuum furnace to  $1500^{\circ}\text{C}$ ; this allowed the inside surface of the crucible to react with the iron. The crucible was then cooled and the iron removed.

A cleaved single crystal of MgO was buried in the iron powder inside the crucible. A recrystallized alumina cover was placed on the crucible; the crucible and cover were wrapped in tantalum foil (which acts as a getter of oxygen) and were placed in the center of the furnace. The system was allowed to pump down to a final pressure of about  $10^{-6}$  torr. The furnace was flushed three times with helium gas to remove oxygen and other gaseous impurities and then was allowed to pump down again to the  $10^{-6}$  torr level. The sample was heated to  $250^{\circ}\text{C}$  for 1 hour, then heated to the final desired temperature for the diffusion runs.

Diffusion runs were made at 1150, 1250, and  $1350^{\circ}\text{C}$  for given lengths of time. Then we used a diamond saw to section a sample; the sample was mounted in plastic and polished by using 600-grit SiC, 1 to 5- $\mu$  diamond, and 0.1- $\mu$  alumina.



MU-32844

Fig. 1. High-temperature furnace.

### A. Electron-Microprobe Analyzer

The polished samples were coated with carbon by vapor deposition to increase their surface electrical conductivity, then mounted in the sample holder for the microprobe. The electron probe scans the surface of the sample with a high-energy electron beam, thereby causing the material present in the sample to emit characteristic x rays. These x rays are monitored by an x-ray spectrometer that indicates the intensity of the  $K_{\alpha}$  x-ray line of the materials present. The samples were scanned at a rate of  $8 \mu/\text{min}$ . The characteristic emissions of both iron and magnesium were monitored. The output of the electron probe supplies a graph that may be converted to a concentration-vs-distance profile if various correction factors are applied.<sup>20-22</sup> It is necessary to correct for such factors as:

- (a) atomic number,
- (b) fluorescence,
- (c) absorption coefficients,
- (d) dead time,

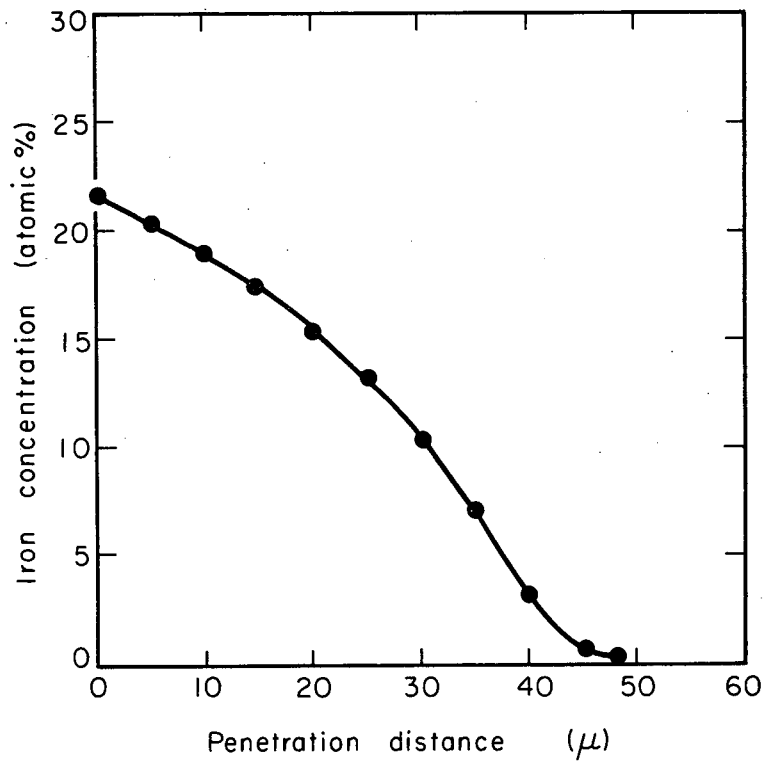
and

- (e) sensitivity.

The corrected data were plotted as concentration of iron in atomic percent vs distance. Figure 2 shows a typical concentration-vs-distance profile obtained from one of the diffusion runs. The shape of the curve was similar to that reported by Rigby in 1962.<sup>9</sup> The curve suggests that the interdiffusion coefficient in the solid-solution series is dependent upon the composition.

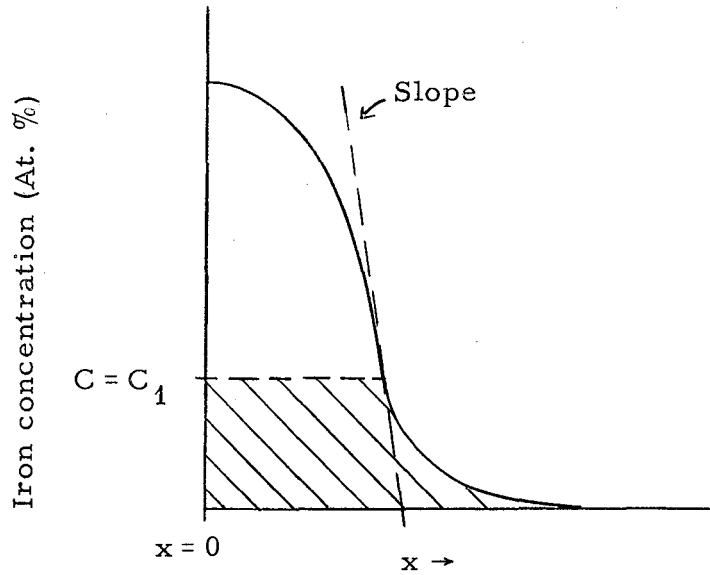
The diffusivity was calculated by using the Boltzmann approach<sup>8</sup> described previously [see Eq. (9)]. The solution of Eq. (9) can be found by using the following graphical analysis:<sup>3</sup> Assuming that the edge of the crystal is our original interface, we can label the profile as shown in the sketch.





MU-32845

Fig. 2. Typical concentration vs distance profile.



We can now obtain the numerical value of  $D$  at any concentration  $C = C_1$  by determining the slope of the curve at that concentration and the area under the curve from  $C = 0$  to  $C = C_1$ , the area in question being the shaded area in the diagram. Knowing  $t$ , the time of diffusion, we can determine  $D$  at any concentration. A computer program was used to evaluate the slopes and area.<sup>23</sup>

#### IV. RESULTS AND DISCUSSION OF RESULTS

The diffusivities calculated for a given temperature were plotted vs iron concentration on a semilog graph, as shown in Figs. 3, 4, and 5. These plots resulted in straight lines from about 1 to 22 at. % iron.

Equations were developed that related the diffusion constant to iron concentration at three temperatures:

for 1150°C, we have

$$D = 8.1 \times 10^{-12} e^{0.150[\text{Fe}]},$$

for 1250°C

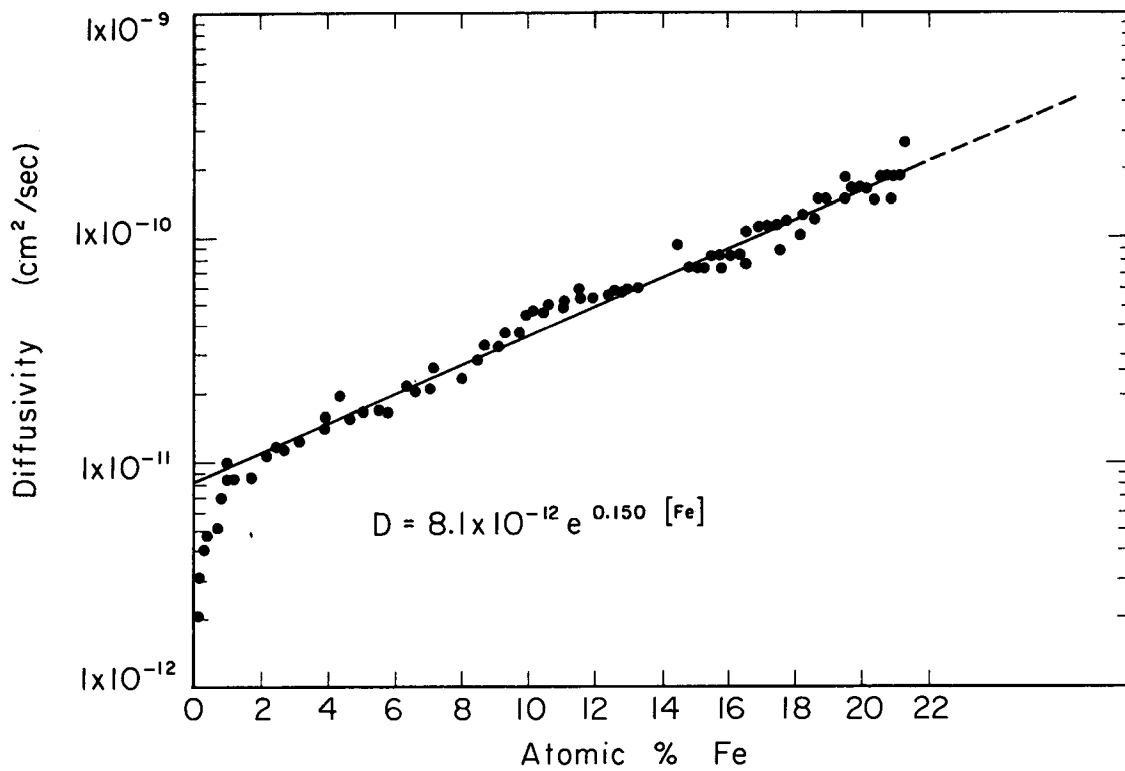
$$D = 1.60 \times 10^{-11} e^{0.173[\text{Fe}]},$$

and for 1350°C

$$D = 2.40 \times 10^{-11} e^{0.190[\text{Fe}]}.$$

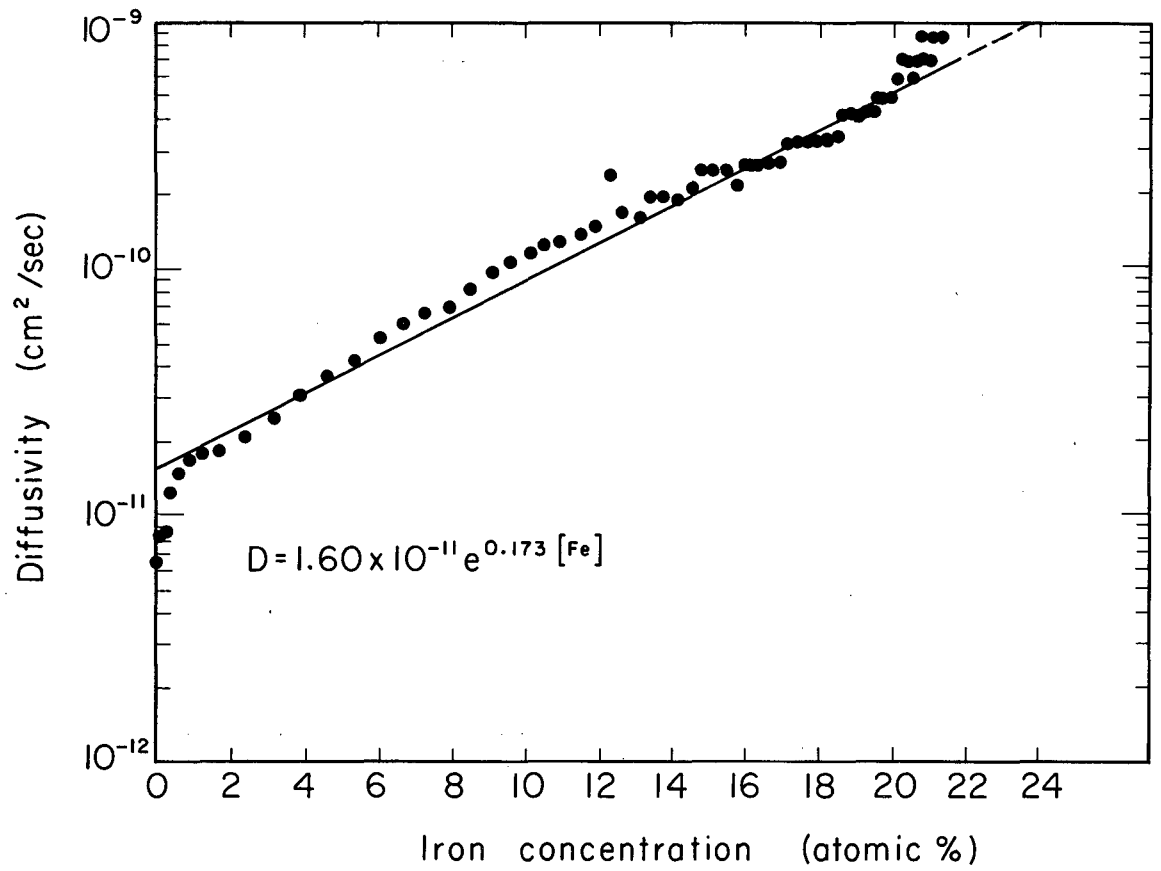
Note that the slope of the line obtained in this manner varies with temperature. The increase in diffusivity as the iron concentration is increased is thought to be caused by an increase in the concentration of vacancies. If the ratio  $\text{Fe}^{+3}/\text{Fe}^{+2}$  remained constant as the iron concentration increased, we would not expect the sharp profile (concentration-vs-distance curve) that is observed. To satisfactorily explain the observed profile, we must assume that the ratio  $\text{Fe}^{+3}/\text{Fe}^{+2}$  not only varies with the iron concentration (as was observed by previous authors) but that the ratio varies exponentially with the iron concentration. Because of an increase in the ratio  $\text{Fe}^{+3}/\text{Fe}^{+2}$  and because of an increase in concentration of  $\text{Fe}^{+2}$ , an increased vacancy concentration will result at higher iron concentrations. This higher vacancy concentration would allow diffusion to proceed at a faster rate and would explain the concentration dependence of the diffusion coefficient.

At this point one might ask how it is known that the  $[\text{Fe}^{+3}]$  increases with iron concentration. In order to determine whether or not the  $[\text{Fe}^{+3}]$  was changing as the iron concentration increased, sections of the diffused sample were cleaved for investigation by electron paramagnetic-resonance techniques (EPR). Two samples were cleaved



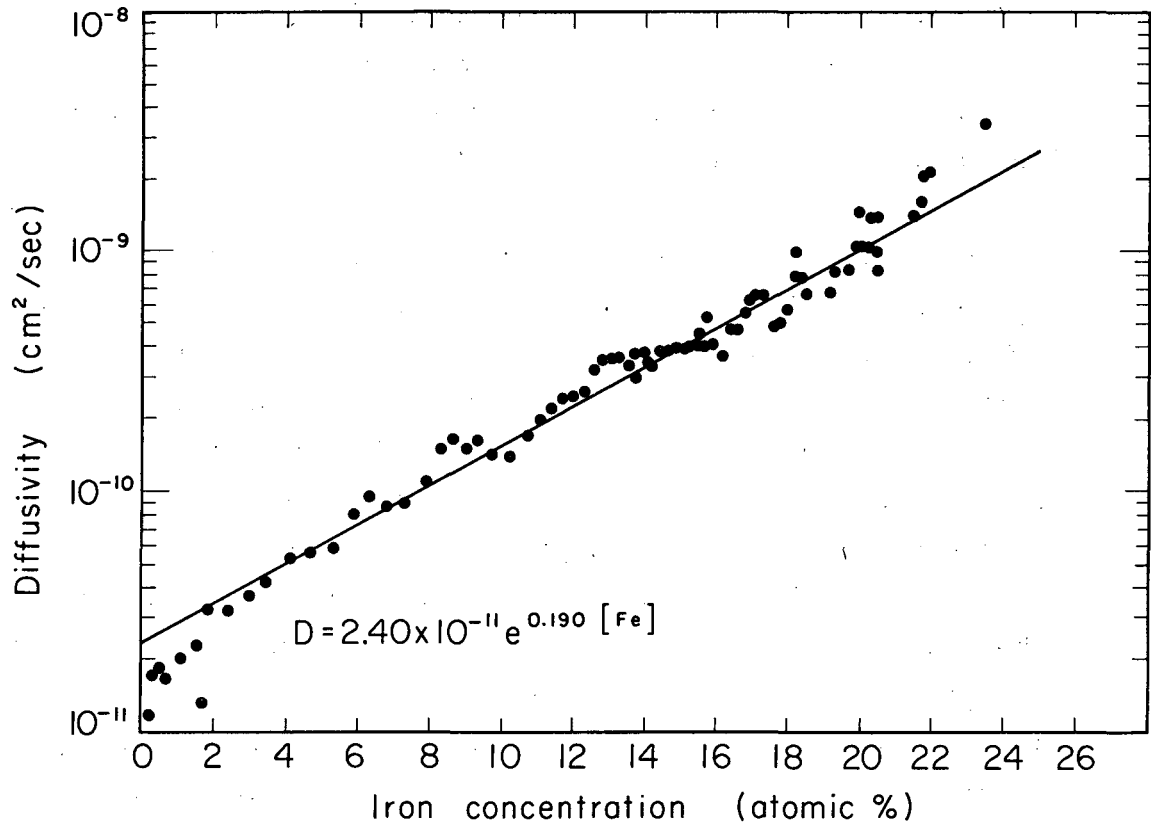
MUB-2279

Fig. 3. Plot of diffusivity vs iron concentration (1150° C).



MUB-2280

Fig. 4. Plot of diffusivity vs iron concentration (1250°C).



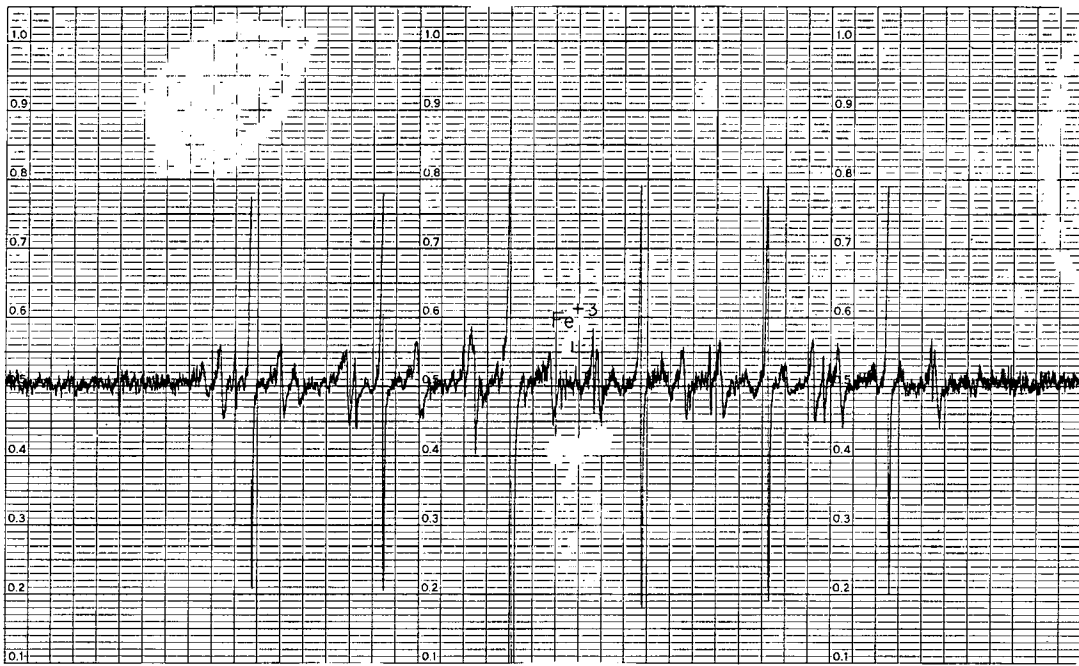
MUB-2281

Fig. 5. Plot of diffusivity vs iron concentration (1350°C).

from a diffused crystal, one from the solid-solution-MgO interface where the concentration of iron was low, and one from the solid-solution-iron interface where the concentration of iron was high. These samples were run in the electron paramagnetic resonance instrument to determine the amount of  $\text{Fe}^{+3}$  present.

The EPR spectra were run at room temperature. The spectrometer was a Varian V-3500 with 100 kc/sec field modulation. On these spectra a plot of the derivative of the absorption curve is shown as a function of the magnetic field. Narrow absorption curves, having large derivative values, are most easily detected by this method. The absolute concentration of a given ion is proportional to the height of the derivative spectrum multiplied by the square of the separation between the derivative peaks. Previous work<sup>24</sup> has shown the  $\text{Fe}^{+3}$  should give a fairly narrow single-line spectrum near  $g = 2.0037$ . The  $\text{Fe}^{+2}$  has been observed only at liquid He temperature, presumably because its absorption is too broad at higher temperatures.

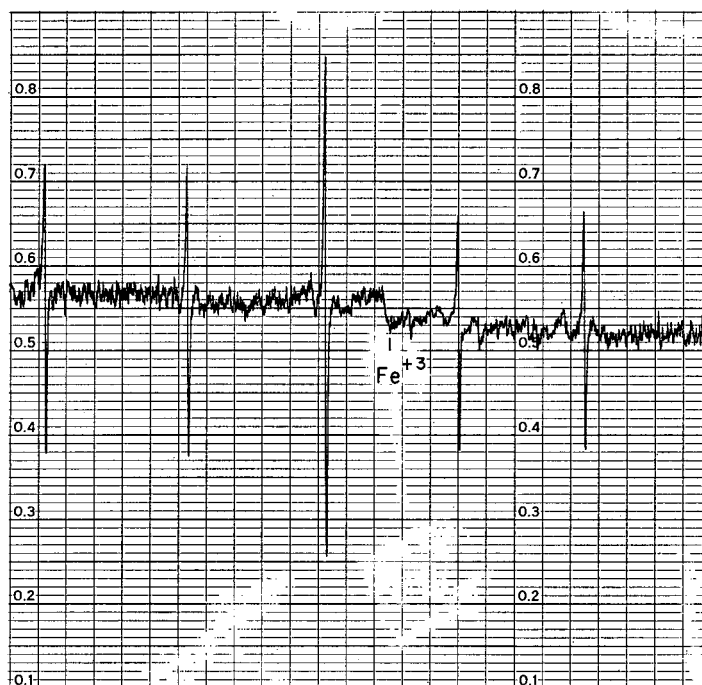
Figures 6, 7, and 8 show the room temperature EPR graphs obtained from the two cleaved samples and from a sample of the original MgO used for diffusion. The six lines observed in all three of the samples are most certainly attributed to  $\text{Mn}^{+2}$  as an impurity in the original MgO crystals. The results of a spectroscopic analysis of the MgO crystals are shown in the Appendix. The small amount of  $\text{Mn}^{+2}$  is observable because of its narrow line width. The sextet for  $\text{Mn}^{+2}$  is centered about a  $g = 2.0014$ . It can be seen by examination of the three graphs that  $\text{Fe}^{+3}$  is essentially absent in the sample of MgO before diffusion (Fig. 6), that a trace is present in the section of the sample closest to the MgO (Fig. 7), and that a noticeable concentration of  $\text{Fe}^{+3}$  exists in the region of higher iron concentration (Fig. 8). Another fact should be noted: In the "pure" MgO sample the background remains constant over the scanned range, while in the samples containing  $\text{Fe}^{+3}$  the background increases as the scanning continues, the degree of increase being related to the iron concentration. It is probable that the  $\text{Fe}^{+2}$  is present but its peak is very broad in the EPR at this temperature.



MU-32846

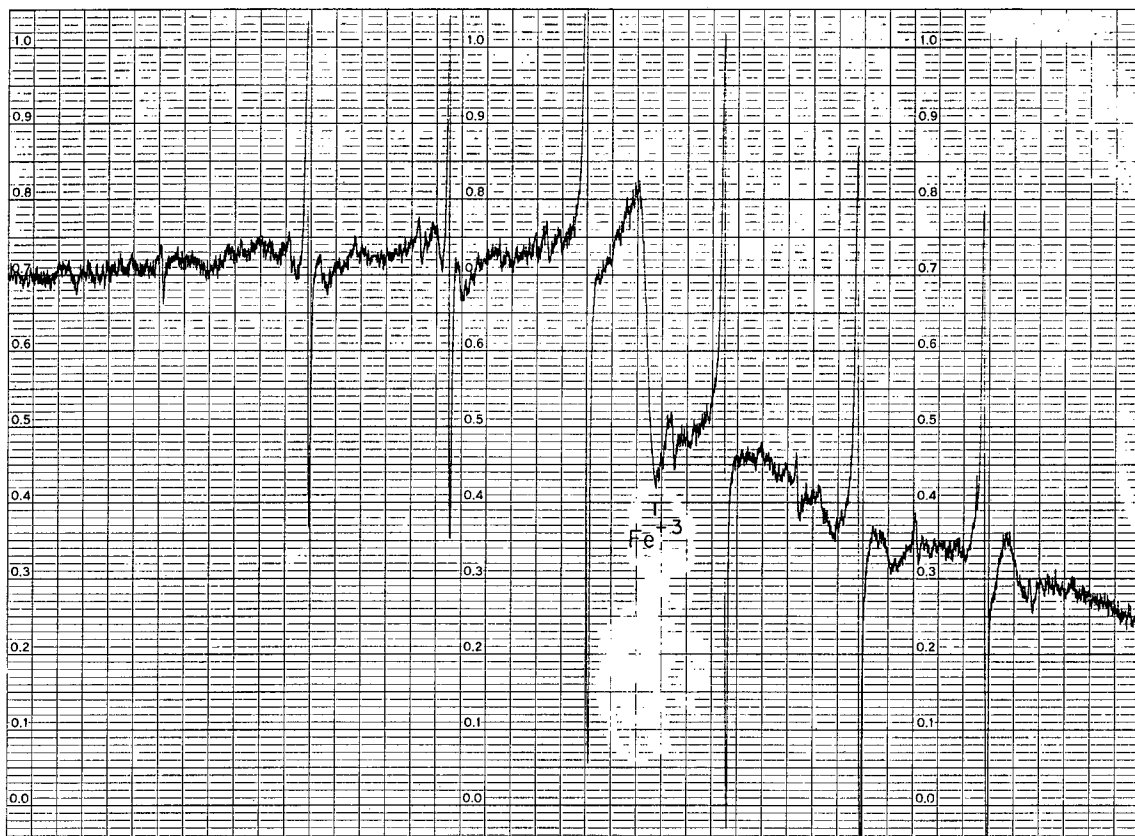
Fig. 6. Electron-paramagnetic resonance of undiffused MgO.





MU-32847

Fig. 7. Electron-paramagnetic resonance of  $\text{Fe}_x\text{O} \cdot \text{MgO}$  section nearest undiffused  $\text{MgO}$ .



MUB-2282

Fig. 8. Electron-paramagnetic resonance of  $\text{Fe}_x\text{O} \cdot \text{MgO}$  nearest iron boundary.

The results of the EPR analysis lend support to the theory that the  $[\text{Fe}^{+3}]$ , and in consequence the vacancy concentration, increases with iron concentration; the results also lend support to the theory that the ratio changes with iron concentration in a nonlinear fashion.

Himmel, Mehl, and Birchenall showed that the diffusivity of iron in  $\text{Fe}_x\text{O}$  was directly proportional to the vacancy concentrations.<sup>13</sup> This present investigation has found that the diffusivity varies exponentially with iron concentration, indicating that the concentration of vacancies increased exponentially with iron concentration. This would require that the ratio  $\text{Fe}^{+3}/\text{Fe}^{+2}$  increases exponentially with iron concentration. A plot of  $\log D$  vs  $1/T$  was made in order to evaluate the activation energy for the process. Figure 9 shows such a plot. It may be observed that at a given iron concentration a straight line is obtained. The equations for the temperature dependence of the diffusivity are as follows:

At  $C = 5$  at. % we have

$$D = 6.34 \times 10^{-7} \exp (-29600 / RT),$$

at  $C = 10$

$$D = 4.49 \times 10^{-6} \exp (-32900 / RT),$$

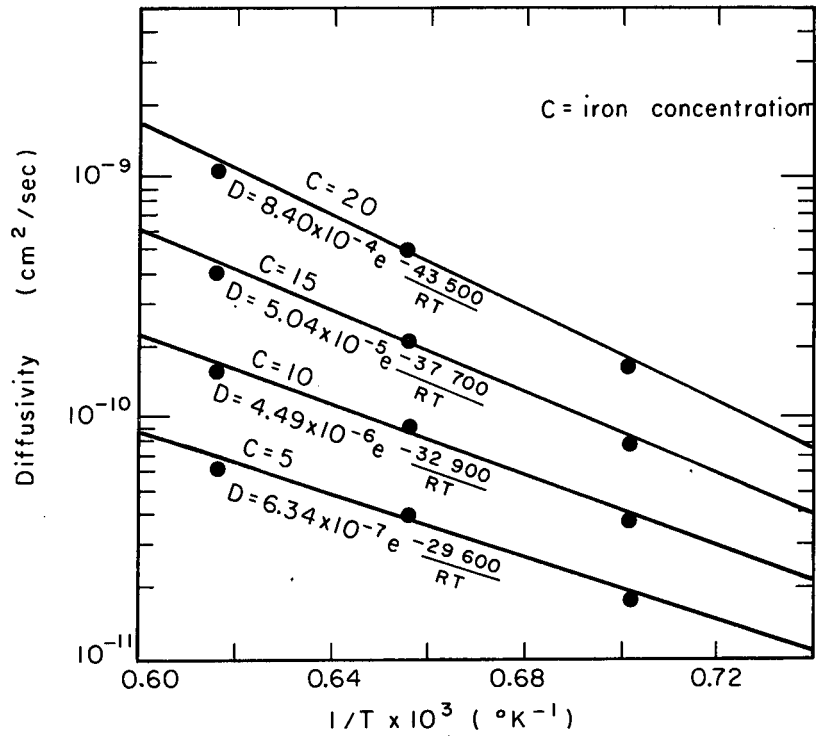
at  $C = 15$

$$D = 5.04 \times 10^{-5} \exp (-37700 / RT),$$

and at  $C = 20$

$$D = 8.40 \times 10^{-4} \exp (-43500 / RT).$$

It is interesting to note that both the slope and the pre-exponential terms increase with increased iron concentration. This seems to indicate that the activation enthalpy varies with composition in the solid-solution region. The variation of the pre-exponential term indicates a variation in entropy with composition, a variation in the ratio  $\text{Fe}^{+3}/\text{Fe}^{+2}$ , or both. It is also interesting to note that Himmel<sup>13</sup> found the same sort of increase in activation energy as the vacancy concentration increased in  $\text{Fe}_x\text{O}$ , but decided that it could have been due to systematic errors in his procedure.



MU-32848

Fig. 9. Diffusivity vs reciprocal temperature for various iron concentrations.

In order to interpret the result of this research, the variation of the ratio  $\text{Fe}^{+3}/\text{Fe}^{+2}$  with temperature must be investigated as a function of iron concentration. If it is found that the temperature dependence of this ratio is concentration-dependent, the observed variation in activation energy could be explained.

## V. CONCLUSIONS

The interdiffusivity in the system iron-MgO is dependent upon the iron concentration. The experimental data obtained for the diffusivity agrees well with the data obtained by previous investigators from studies of the diffusion of  $\text{Fe}_x\text{O}$  in MgO,<sup>9</sup> indicating that the reaction between Fe and MgO is rapid and not rate-controlling in relation to the diffusion process. The diffusivity shows an exponential increase with iron concentration in the composition range 1 to 22 at. % iron. The activation energy for the process was also found to increase with increase of the iron concentration.

#### ACKNOWLEDGMENTS

I thank Professor J. A. Pask for his direction of this research project. Professor A. W. Searcy, Professor R. M. Fulrath, Professor L. Brewer, Professor J. E. Dorn, and Professor R. J. Myers have been sources of counsel for which I am grateful. I thank Dr. B. Evans, Department of Geology, for his kind assistance in the electron microprobe studies, and Mr. B. Spencer for his assistance in the electron paramagnetic resonance analysis. Thanks are also given to Mrs. Bette Blank and Mr. R. Rossi for their helpful discussions and to the staff of the Lawrence Radiation Laboratory's Inorganic Materials Research Division.

This work was done under the auspices of the U. S. Atomic Energy Commission.

APPENDIX

Results of a spectroscopic analysis of the MgO single crystals before diffusion.

Impurity	%
Fe	0.01
Mn	0.0015
Al	0.005
Cu	0.0015
Ni	-
Ca	0.01
Cr	0.001
Si	-
B	-
Total impurities	0.0290 %

Analysis done by American Spectrographic Laboratories,  
San Francisco



FOOTNOTES AND REFERENCES

1. C. Wagner, Diffusion and High-Temperature Oxidation of Metals, Symposium, Atom Movements (American Society of Metals, Cleveland, Ohio 1951), p. 153.
2. A. B. Lidiard, Ionic Conductivity, Handbuch der Physik, 20, 246 (1957).
3. J. Crank, Mathematics of Diffusion (Clarendon Press, Oxford, 1956).
4. W. Jost, Diffusion in Solids, Liquids and Gases (Academic Press, New York, 1931).
5. W. D. Kingery, Atom Mobility, in Introduction to Ceramics (John Wiley and Sons, Inc., New York, 1960), p. 217.
6. R. M. Barrer, Diffusion In and Through Solids (MacMillan Co., New York, 1931).
7. C. E. Birchenall, The Mechanism of Diffusion in the Solid State, Met. Revs. 3, 235 (1958).
8. L. Boltzmann, Ann. Physik, Leipzig, 53, 959 (1894).
9. E. B. Rigby, Diffusion of Wustite into Single Crystals of Periclase, Ph.D. Thesis, University of Utah, 1962.
10. A. B. Lidiard, Impurity Diffusion in Crystals, Phil. Mag. 46, 1218 (1955).
11. B. J. Wuench and T. Basilos, Diffusion of Transition Metal Ions in Single-Crystal MgO, J. Chem. Phys. 36, 2917 (1962).
12. S. Glasston, K. J. Laidler, and H. Eyring, The Theory of Rate Processes (McGraw-Hill Book Co., Inc., New York, 1941).
13. L. Himmel, R. F. Mehl, and C. E. Birchenall, Self-Diffusion of Iron in Iron Oxides and the Wagner Theory of Oxidation, Inst. Min. Met. Eng., 197, 827 (1953).
14. R. E. Carter and R. D. Richardson, An Examination of the Decrease of Surface Activity Method of Measuring Self Diffusion Coefficients in Wustite and Cobaltous Oxide, Trans. AIME 200, 1244 (1954).

15. E. R. Jette and F. Foote, A Study of the Homogeneity Limits of Wustite by X-Ray Methods, *Trans. AIME* 105, 276 (1933).
16. A. F. Wells, Structural Inorganic Chemistry (Clarendon Press, Oxford, 1950), 2nd ed.
17. R. Linder and G. D. Parfitt, Diffusion of Radioactive Magnesium in Magnesium Oxide Crystals, *J. Chem. Phys.* 26 (1) 482 (1957).
18. N. L. Bowen and J. F. Schairer, The System MgO-FeO-SiO<sub>2</sub>, *Am. J. Sci.*, 5th Series, 29, 151 (1935).
19. J. Brynstad and H. Flood, The Redox Equilibrium in Wustite and Solid Solutions of Wustite and Magnesium Oxide, *Z. Elektrochem* 62, 953 (1958).
20. Using tables (unpublished) by I. Adler, which uses R. Castaing's experimental absorption correction curves and theoretical formula of J. Philibert.
21. R. Castaing, Electron Probe Microanalysis, in Advances in Electronics and Electron Physics XIII (Academic Press, New York, 1960), pp. 317-386.
22. J. Philibert, The Castaing Microsonde in Metallurgical and Mineralogical Research, *J. Inst. Metals* 90, 241-52 (1961-2).
23. TRAPSL (A. Z) Lawrence Radiation Laboratory, Berkeley, laboratory routine program for calculating diffusivities.
24. W. Low, Paramagnetic Resonance in Solids (Academic Press, New York, 1960), p. 119.

This report was prepared as an account of Government sponsored work. Neither the United States, nor the Commission, nor any person acting on behalf of the Commission:

- A. Makes any warranty or representation, expressed or implied, with respect to the accuracy, completeness, or usefulness of the information contained in this report, or that the use of any information, apparatus, method, or process disclosed in this report may not infringe privately owned rights; or
- B. Assumes any liabilities with respect to the use of, or for damages resulting from the use of any information, apparatus, method, or process disclosed in this report.

As used in the above, "person acting on behalf of the Commission" includes any employee or contractor of the Commission, or employee of such contractor, to the extent that such employee or contractor of the Commission, or employee of such contractor prepares, disseminates, or provides access to, any information pursuant to his employment or contract with the Commission, or his employment with such contractor.